SHOCK, Vol. 59, No. 6, pp. 902–911, 2023

OPEN

THE IL-33/ST2 AXIS PROMOTES ACUTE RESPIRATORY DISTRESS SYNDROME BY NATURAL KILLER T CELLS

Lijuan Zou,*† Wenpei Dang,*† Yiming Tao,*† Hui Zhao,*† Bin Yang,*† Xinxin Xu,*† and Yongsheng Li*†

**Department of Intensive Care Medicine, Tongji Hospital, Tongji Medical College, Huazhong University of Science and Technology, Wuhan, China; and †The Emergency Department, Tongji Hospital, Tongji Medical College, Huazhong University of Science and Technology, Wuhan, China*

Received 21 Dec 2022; first review completed 11 Jan 2023; accepted in final form 24 Feb 2023

ABSTRACT—Acute respiratory distress syndrome (ARDS) is characterized by uncontrolled inflammation, which manifests as leukocyte infiltration and lung injury. However, the molecules that initiate this infiltration remain incompletely understood. We evaluated the effect of the nuclear alarmin IL-33 on lung damage and the immune response in LPS-induced lung injury. We established a LPS-induced lung injury mouse model. We used genetically engineered mice to investigate the relationship among the IL-33/ST2 axis, NKT cells, and ARDS. We found that IL-33 was localized to the nucleus in alveolar epithelial cells, from which it was released 1 h after ARDS induction in wild-type (WT) mice. Mice lacking IL-33 (IL-33$^{-/-}$) or ST2 (ST2$^{-/-}$) exhibited reduced neutrophil infiltration, alveolar capillary leakage, and lung injury in ARDS compared with WT mice. This protection was associated with decreased lung recruitment and activation of invariant nature killer (iNKT) cells and activation of traditional T cells. Then, we validated that iNKT cells were deleterious in ARDS in CD1d$^{-/-}$ and Vα14Tg mice. Compared with WT mice, Vα14Tg mice exhibited increased lung injury in ARDS, and the CD1d$^{-/-}$ mice showed outcomes opposite those of the Vα14Tg mice. Furthermore, we administered a neutralizing anti-ST2 antibody to LPS-treated WT and Vα14Tg mice 1 h before LPS administration. We found that IL-33 promoted inflammation through NKT cells in ARDS. In summary, our results demonstrated that the IL-33/ST2 axis promotes the early uncontrolled inflammatory response in ARDS by activating and recruiting iNKT cells. Therefore, IL-33 and NKT cells may be therapeutic target molecules and immune cells, respectively, in early ARDS cytokine storms.

KEYWORDS—Interleukin 33; lung injury; acute respiratory distress syndrome; inflammation; invariant natural killer T cells

INTRODUCTION

Acute respiratory distress syndrome (ARDS) is a common clinical condition that occurs in response to various inciting stimuli. It has a high morbidity rate, up to 10% (1), and a high mortality rate, up to 45%–57.8% (2), in intensive care units. Despite decades of research, no effective drug therapies are available for ARDS. The probable explanation for the failure to obtain effective therapy includes deficits in our understanding of ARDS pathogenesis, which is extremely complicated. It is now widely accepted that a variety of molecular mechanisms are involved in ARDS, but the core molecular in ARDS is still unknown.

IL-33 is a newly discovered member of the IL-1 family that releases an alarm signal to immune cells expressing the ST2 receptor in response to cell injury or tissue damage (3). It is expressed in various cell types (4,5), mainly endothelial cells and airway epithelial cells. Serum IL-33 increases in patients with ARDS (6). IL-33 production increases with disease severity (7,8) and independently predicts poor prognosis in ARDS (9,10) and COVID-19 (9,11). Turnquiast's experiment indicated that IL-33 stimulated Tregs to secrete IL-13 to control myeloid responses and inflammation after lung injury in mouse models of resuscitation-related hemorrhagic shock and tissue trauma (12). In CLP-induced sepsis, IL-33 regulates IL-5 but not ILC2s, leading to local inflammation in the lungs (13). However, IL-33 may also initiate early detrimental type 2 immune responses after trauma through ILC2 regulation of neutrophil IL-5 production (14). Its conversion to the alarmin and the mechanism through which IL-33 regulates the immune response needs further investigation.

NKT cells are innate immune cells that are powerful producers of various cytokines and antimicrobial molecules (15). NKT cells express ST2, which is an IL-33 receptor (16). Therefore, NKT cells may be affected by IL-33 *via* the IL-33/ST2 axis. IL-33 activated iNKT cells 1 h after transplantation (17) and in asperamide B-induced asthma (18). Moreover, spleen and liver iNKT cell counts increased twofold, after a treatment of mice with IL-33 (19). In addition, IL-33 directly targeted iNKT cells and promoted iNKT cell recruitment and cytokine production after kidney ischemia-reperfusion injury (IRI) (20). According to these studies, IL-33 contributes to NKT cell recruitment, activation, and cytokine production in asthma, ischemia-reperfusion injury (IRI), and transplantation. However, whether IL-33 promotes iNKT cell recruitment to promote lung injury in ARDS is still unknown.

Herein, to elucidate whether IL-33 can promote an uncontrolled inflammatory response in the early stage of ARDS by activating NKT cells, we assessed their role in NKT cell using genetically engineered mice and rescue experiments. Our results showed that the IL-33/ST2 axis promoted an early uncontrolled inflammatory response in ARDS that depended on NKT cells.

Address reprint requests to Yongsheng Li, Department of Intensive Care Medicine and the Emergency Department, Tongji Hospital, Tongji Medical College, Huazhong University of Science and Technology, No. 1095, Jiefang Ave, Qiaokou District, Wuhan, 430040, Hubei, China. E-mail: tjh_ysli@163.com

This work was supported by the Chen Xiao-ping Foundation for the Development of Science and Technology of Hubei Province (no. CXPJJH12000005-07-40) and the Beijing Medical and Health Foundation (BXS5-22001).

The authors report no conflicts of interest.

Ethics approval was obtained from the Tongji Hospital Committee for the Ethical Approval of Research Involving Animals.

DOI: 10.1097/SHK.0000000000002114

MATERIALS AND METHODS

Mice

Male 6- to 8-week-old C57BL/6 mice were purchased from GemPharmatech (Jiangsu, China). IL-33$^{-/-}$, ST2$^{-/-}$, CD1d$^{-/-}$ mice (NKT cell–deficient), and Vα14-Jα18 transgenic (Vα14Tg, increased NKT cells) all with a C57BL/6 background were kindly provided by the Immunology Laboratory of Tongji Medical College of Huazhong University of Science and Technology. All the animals were housed and maintained under specific pathogen-free conditions in our animal facility. The Institutional Animal Care and Use Committee of the Academic Medical Center approved and reviewed all procedures.

The ARDS models

Mice of similar weight mice were selected and anesthetized with sodium pentobarbital (50 mg/kg intraperitoneally) and administered an intratracheal injection with 20 mg/kg LPS (L2880, Sigma-Aldrich, St Louis, MO) in 50 μL of PBS or 50 μL of PBS as the control treatment. To block endogenous IL-33 activity, a recombinant mouse ST2 Fc chimera or a recombinant human (immuneglobulin G) IgG1 Fc as the control (5 μg per mouse) (R&D Systems, Abingdon, United Kingdom) was administered to ARDS-treated mice 1 h before LPS administration. The mice were killed 24 h after the LPS or control injection. Lung tissues, blood, BALF, and the spleen were removed for further study. After coagulation at room temperature for 1 h, the blood was centrifuged at 1,500*g* at 4°C for 10 min.

Flow cytometry

The lung tissue and spleen were collected to prepare a single-cell suspension. Single cells were incubated with anti-CD45, anti-CD11b, anti-ly6G, anti-CD69 (BD, NJ), anti-CD1d-tetramer (a-Gelcer loaded-PE; MBL, Japan), anti-CD3 (Bioscience, Tian Jin, China), and anti-CD11b antibodies for 40 min at 4°C. The cells were washed once with FACS buffer (PBS + 2% FBS). Flow cytometry was performed on a CytoFLEX S instrument (Beckman Coulter, Inc), and all data were analyzed with FlowJo software v10.8.1.

ELISAs

According to the manufacturer's instructions, IL-33 concentrations in mouse serum and lung tissue were tested using ELISA kits (R&D Systems, Abingdon, United Kingdom).

Western blotting

After mechanical tissue disruption, lung tissue was homogenized on ice in RIPA buffer (Servicebio, Wuhan, China) containing protease inhibitors and phosphatase inhibitors (Servicebio, Wuhan, China) for 30 min, according to the manufacturer's instructions. Then, 5× NaDodSO4 loading buffer (Servicebio, Wuhan, China) was added to all samples and heated for 15 min at 98°C. Next, the samples were separated by 10% sodium dodecyl sulfate-polyacrylamide gel electrophoresis before being transferred to polyvinylidene difluoride membranes. After blocking with 5% nonfat milk for 2 h at room temperature, the membranes were incubated overnight at 4°C with primary Abs against β-actin (1:2,000, ABclonal, Wuhan, China), GAPDH (1:2,000, ABclonal, Wuhan, China), IL-33 (1:1,000, R&D Systems, Abingdon, United Kingdom), and ST2 (1:1,000, Proteintech, Wuhan, China). The membranes were then incubated with horse radish peroxidase(HRP)-linked anti-goat IgG (1:7,000, ABclonal, Wuhan, China) for 1 h at room temperature. The immunoreactive protein was visualized with an ECL detection reagent (MCE, NJ).

Immunohistochemistry

Paraformaldehyde-fixed, paraffin-embedded sections were deparaffinized and rehydrated, and antigen retrieval was performed by microwave heating of the sections in citric acid (pH 6) for 10 min, followed by incubation with 3% H_2O_2 for 5 min to inhibit endogenous catalase. Then, the sections were washed three times with TBS with 0.1% Tween 20 for 5 min, blocked with 3% BSA for 1 h at room temperature, and incubated overnight at 4°C with IL-33 (1:200 R&D Systems). Next, the sections were washed three times in TBS with 0.1% Tween 20 for 5 min, incubated with 10 mg/mL HRP-linked donkey anti-goat IgG (Proteintech) antibody for 1 h at room temperature, incubated with diaminobenzidine for 1 min, and then stained with hematoxylin for 30 s. All images were obtained with an Olympus microscope BX51.

Quantitative real-time PCR

Lung tissue RNA was extracted using TRIzol (Ambion) after lysis and reverse transcribed into cDNA using a reverse transcription kit (Tsingke Biotechnology Co, Ltd, Beijing, China) according to the manufacturer's instructions. The expression levels of the target genes IL-33 and GAPDH were detected by SYBR Green quantitative real-time PCR (Toyobo, Osaka, Japan). The relative gene expression was calculated using the 2-detla-detla Ct method. The primer sequences were IL-33 (forward, 5′-TCCAACTCCAAGATTTCCCCG-3′; reverse, 5′-TTATGGTGAGGCCAGAACGG-3′) and GAPDH (forward, 5′-ACTCTTCCACCTTCGATGCC-3′; reverse, 5′-TGGGATAGGGCCTCTCTTGC-3′).

Lung inflammation assays

Bronchoalveolar lavage and protein measurement

The right lungs were flushed three times *in situ* with 0.4 mL of ice-cold sterile saline (0.9% NaCl). BALF was centrifuged (300*g*, 5 min), cells were collected for flow analysis, and the supernatant was frozen (−80°C) until use for further analysis. A bicinchoninic acid assay (Servicebio, Wuhan, China) was used to determine the total protein in the BALF.

Lung dry/wet ratio

The wet weight of the lung tissue was measured before desiccation at 60°C for 48 h. The dry/wet weight ratio (D/W) was calculated after desiccation.

Histological analysis

The right lung lobes were fixed in 4% paraformaldehyde (Servicebio, Wuhan, China) at room temperature. The samples were then dehydrated and embedded in paraffin. Sections were cut into 4-μm sections and stained with hematoxylin-eosin for histological analysis. Lung injury of the sections was scored on the basis of four categories (alveolar and interstitial edema, alveolar and interstitial hemorrhage, alveolar and interstitial inflammation, and atelectasis), from 0 (normal) to 4 (severe): 0 = no damage, 1 = damage up to 25% of the field, 2 = damage up to 25%–50% of the field, 3 = damage to 50%–75% of the field, and 4 = diffused damage. The severity of the lung injury was analyzed by two pathologists blinded to the experimental group based on 10 randomly selected high-power fields (400×) in each section.

CBA

A CBA Mouse inflammation kit (BD Biosciences, San Jose, CA) was used to measure IL-6, IL-10, and MCP-1 concentrations in sera and BALF according to the manufacturer's instructions. The lower detection limits were 5, 17.5, and 52.7 pg/mL, respectively.

Statistical analysis

The data are presented as the mean ± standard deviation (SD). The data were analyzed using GraphPad Prism version 8.3.1 (GraphPad Software, La Jolla, CA). An unpaired two-tailed Student *t* test was performed to compare two groups, and one-way ANOVA was used for comparisons among multiple groups when the data were normally distributed. A nonparametric test was used when the data did not follow a normal distribution. A *P* value less than 0.05 was considered to be statistically significant (*$P < 0.05$, **$P < 0.01$, ***$P < 0.001$, and ****$P < 0.0001$).

RESULTS

IL-33 is elevated 1 h after LPS-induced lung injury

We first assessed whether IL-33 participated in LPS-induced lung injury. The mRNA and protein expression levels of IL-33 were detected by qPCR, ELISA, and western blotting. The mRNA level of IL-33 was significantly increased at 1 h in the model lung tissue 1 h after ARDS induction and decreased at 3 and 24 h compared with that in the control group (Fig. 1A), $P < 0.05$). ELISA and western blot analysis confirmed the results (Fig. 1, C–E). Moreover, there was concomitant with a rise in IL-33 in the BALF (Fig. 1B), which was negligible in the control group and increased at 1 h but decreased at 3 and 24 h after ARDS induction of the models. We also detect the concentration of ST2 by western blot analysis. The concentration of ST2 increases gradually and was significantly increased at 24 h in lung tissue after ARDS induction compared with that in the control group (Fig. 1, G–H, $P < 0.05$). Immunohistochemistry staining was performed to detect IL-33 localization in the lung. As shown in Figure 1F, alveolar-type epithelial cells expressed IL-33 predominantly in their nuclei in the wild-type (WT) ARDS mice compared with IL-33$^{-/-}$ mice.

Mice lacking IL-33 or its specific receptor ST2 were protected against ARDS

Then, we tried to confirm the role played by the IL-33/ST2 axis in ARDS by measuring lung alveolar capillary leakage,

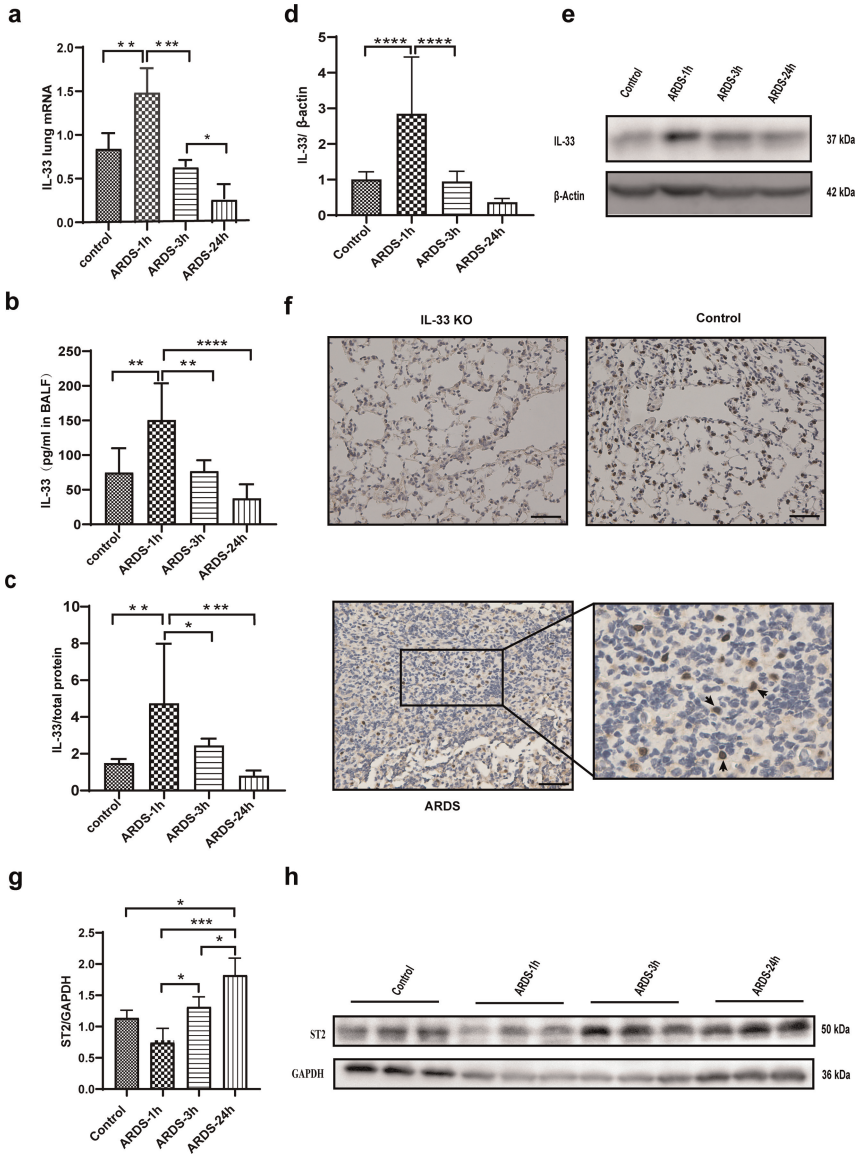

FIG. 1. **IL-33 increased in the lung and BALF 1 h after LPS-induced lung injury.** WT mice were administered an intratracheal injection of LPS, and then the lung tissue and BALF were collected for 1, 3, and 24 h after ARDS induction. A, The mRNA expression level of IL-33 was detected by quantitative polymerase chain reaction (n = 5). In the BALF (B) and lung (C), IL-33 protein concentrations were determined *via* ELISA (n = 5–8) and western blotting (E–D) (n = 5–8). Total protein in the lung (C) was measured by BCA. F, An anti-IL-33 antibody was used for the immunohistochemistry analysis of lung tissue (n = 5). IL-33^{-}/$^{-}$ mice were used as the negative controls. Arrowheads point to the nuclear translocation of IL-33. Scale bar = 50 μm. G, Lung protein concentrations in lung tissue were determined *via* western blotting (n = 3), and (H) was the typical picture. The results are shown as the mean + SD. *$P < 0.05$, **$P < 0.01$, ***$P < 0.001$, ****$P < 0.0001$, and n. s., not significant. ARDS, acute respiratory distress syndrome; BALF, bronchoalveolar lavage fluid; and KO, knockout; WT, wild-type.

pulmonary edema, and lung tissue damage in WT, IL-33^{-}/$^{-}$, and ST2^{-}/$^{-}$ mice 24 h after ARDS model establishment. To evaluate alveolar capillary leakage and pulmonary edema, we measured the ratio of the D/W, total protein concentration, and neutrophil infiltration in the BALF. After LPS-induced lung injury, we found that the D/W ratio decreased and that the total protein concentration and neutrophil infiltration increased in WT mice (Fig. 1, A–C). However, the D/W ratio was significantly increased in the IL-33^{-}/$^{-}$ and ST2^{-}/$^{-}$ groups compared with the WT-ARDS group ($P < 0.05$; Fig. 2A). The number of neutrophils in the BALF decreased in the IL-33KO group and ST2KO group ($P < 0.05$; Fig. 2, B–C), but there was no difference in the protein concentration in the BALF between the ST2 KO group and WT ARDS group (Fig. 2B). Simultaneously, under a light microscope, HE staining of the control group showed normal lung structures. After LPS-induced lung injury, leukocyte infiltration, alveolar congestion/hemorrhage, alveolar collapse, and thickened alveolar walls were observed in the lung tissues of the WT ARDS group (Fig. 2D). The IL-33^{-}/$^{-}$ and ST2^{-}/$^{-}$ ARDS groups showed less morphological damage in the lungs than the ARDS group, as indicated by decreased leukocyte infiltration, alveolar congestion/hemorrhage, alveolar collapse, and thickened alveolar walls (Fig. 2D). The lung injury scores showed that lacking IL-33 or its specific receptor ST2 alleviated the lung inflammatory response (Fig. 2E).

Mice lacking IL-33 or its specific receptor ST2 exhibit decreased proinflammatory cytokine secretion

In addition, CBA was performed to further assess the systemic inflammatory role of the IL-33/ST2 axis in ARDS and to measure the protein concentrations of IL-6, MCP-1, and TNF in the BALF

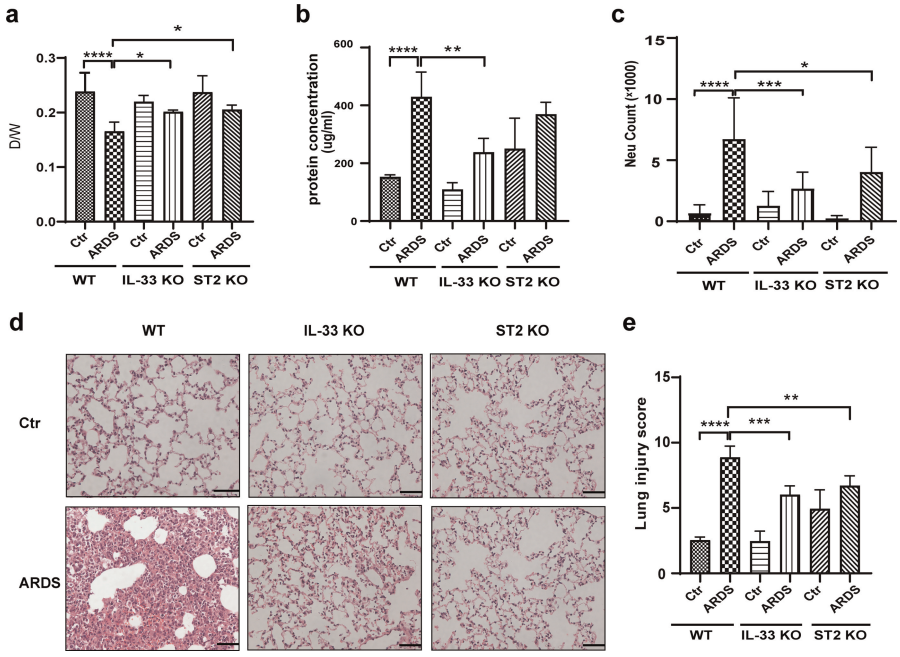

FIG. 2. **The IL-33/ST2 axis promotes lung damage in LPS-induced ARDS.** BALF and lung tissue were harvested after LPS administration for 24 h. A, The lung D/W ratio was assessed to evaluate lung edema (n = 5). B, Protein concentration and neutrophil count (C) in the BALF were analyzed with a BCA kit and flow cytometry to detect epithelial permeability (n = 5). D and E, Histopathological images of the lung tissues are based on one representative image among five (HE staining), and the scale bar = 50 μm. The results are shown as the mean + SD. *$P < 0.05$, **$P < 0.01$, ***$P < 0.001$, ****$P < 0.0001$, and n. s., not significant. ARDS, acute respiratory distress syndrome; BALF, bronchoalveolar lavage fluid; ctr, control; D/W, dry/wet; HE, hematoxylin-eosin; KO, knockout; WT, wild-type.

and serum at 24 h after ARDS induction. As expected, LPS-induced ARDS resulted in marked increases in IL-6, MCP-1, and TNF levels both in the plasma (Fig. 3A) and BALF (Fig. 3B) after 24 h. The serum and BALF levels of these cytokines were significantly lower in the ST2−/− mice. The same outcome regarding the concentration of these cytokines in serum was observed in IL-33$^{-/-}$ mice. However, the BALF levels of IL-6 and TNF were not different in the mice lacking IL-33 (Fig. 3B).

Lung iNKT cell recruitment and activation are impaired in IL-33– or ST2-deficient mice

The data showed that the IL-33/ST2 axis plays a detrimental role in mice with ARDS. Here, we further explored whether IL-33 induces an uncontrolled inflammatory response *via* iNKT cells and can be activated and recruited to inflammatory lung tissue by IL-33 iNKT cells (8). To this end, we examined whether IL-33 or ST2 deficiency affected iNKT recruitment and activation 24 h after

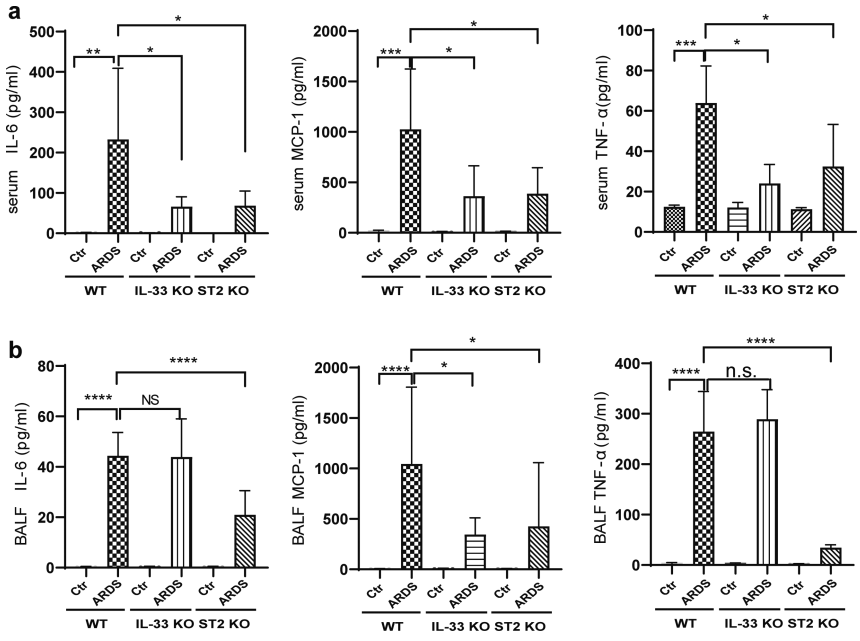

FIG. 3. **IL-33 and ST2 deletion leads to reduced levels of circulating and BALF proinflammatory cytokines.** The concentrations of cytokines in the serum and BALF were measured 24 h after ARDS induction and by CBA. The IL-6, MCP-1, and TNF levels in the plasma (A) and BALF (B) of WT mice, IL-33$^{-/-}$ mice, and ST2$^{-/-}$ mice were measured to evaluate the systemic inflammatory response (n = 5). The data are shown as the mean + SD *$P < 0.05$, **$P < 0.01$, ***$P < 0.001$, ****$P < 0.0001$, and n. s., not significant. ARDS, acute respiratory distress syndrome; BALF, bronchoalveolar lavage fluid; CBA, bead-based multiplex immunoassay; ctr, control; KO, knockout; WT, wild-type.

ARDS induction. As shown in Figure 4C, the ratio of iNKT cells ($CD45^+CD3^+CD1dTT^+$) (Fig. 4A) to $CD3^+$ T lymphocytes was markedly increased in the LPS-induced ARDS group compared with the WT ARDS group in the lung, while no difference in the spleen was found. Moreover, the geometric mean of CD69 surface expression on iNKT cells (Fig. 4, B and C) was markedly increased, which reflected its activation by LPS. IL-33 and ST2 deficiency significantly decreased the iNKT cell frequency and the geometric mean of CD69 abundance in the lung (Fig. 4C). Although spleen iNKT cells showed no difference in frequency (Fig. 4C) in the IL-33 $^{-/-}$ mice and $ST2^{-/-}$ mice, the geometric mean of CD69 expression on iNKT cells decreased compared with that in WT mice (Fig. 4C). After LPS administration *via* the airway, the ratio of NK cells ($CD45^+CD3^-NK1.1^+$) (Fig. 4D) to $CD3^-$T cells was increased in the lung and decreased in the spleen (Fig. 4F). However, the geometric mean of CD69 cell surface expression (Fig. 4E) was not different in the lung but was markedly decreased in the spleen (Fig. 4F). Notably, in both the lung and spleen, IL-33 and ST2 deficiency did not affect the ratio of NK cells to CD3-T cells or the expression of CD69 on NK cells (Fig. 4F).

Conventional T-cell activation is impaired in IL-33– and ST2-deficient mouse

The number of iNKT cells, unconventional T cells, was decreased in IL-33– and ST2-deficient mice. Therefore, we measured the percentage of conventional T cells in ARDS to evaluate their role 24 h after ARDS induction. As shown in Figure 5A, the number of $CD4^+$ T cells ($CD45^+CD3^+CD4^+$) was markedly decreased in the ratio of $CD4^+$ T cells to $CD3^+$ T lymphocytes (Fig. 5A), and the geometric mean of CD69 cell surface expression (Fig. 5A) was increased in the lung and spleen in the LPS-induced ARDS group. Moreover, IL-33 and ST2 deficiency significantly decreased the geometric mean of CD69 expression on $CD4^+$ T cells in the lung. ST2 deficiency significantly increased the ratio of $CD4^+$ T cells to $CD3^+$ T lymphocytes (Fig. 5A). However, no difference in the ratio of $CD4^+$ T cells to $CD3^+$T cells or in the geometric mean of CD69 cell surface expression in the spleen of IL-33– or ST2-deficient mice was found. The number of $CD8^+$ T cells ($CD45^+CD3^+CD8^+$) was markedly increased in the ratio of $CD8^+$ T cells to $CD3^+$ T lymphocytes (Fig. 5B) in the spleen of mice with LPS-induced ARDS. However, no difference was found in the lung. The geometric mean

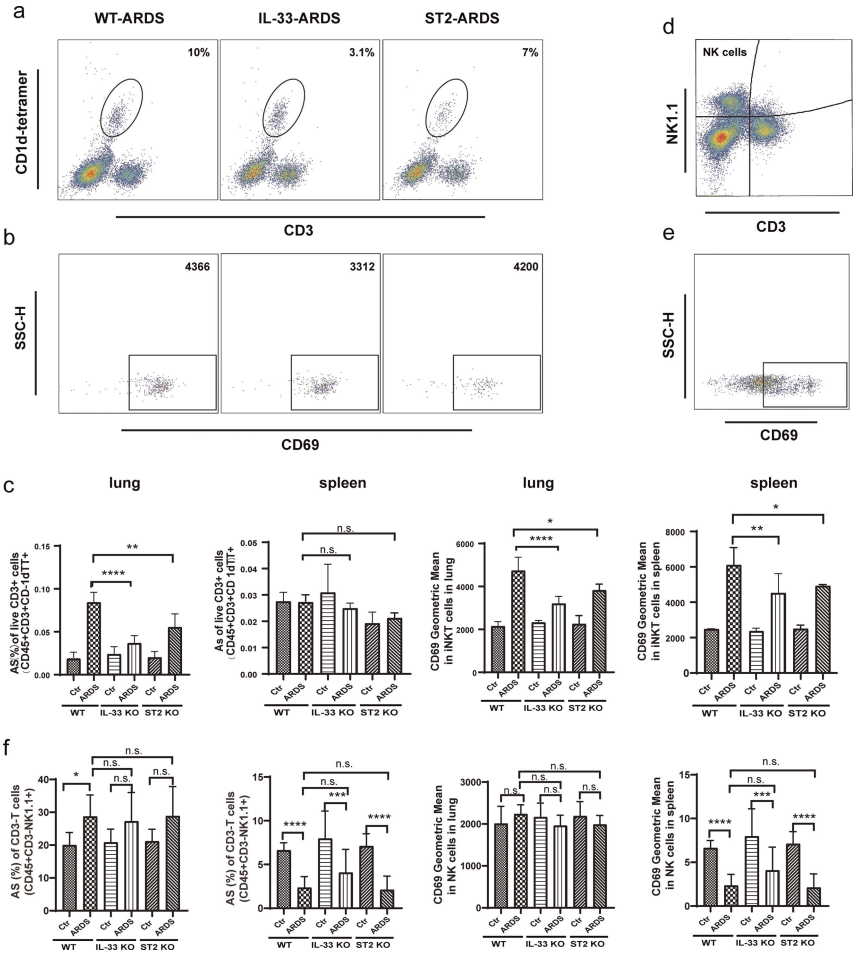

FIG. 4. **Mice lacking IL-33 and ST showed reduced ability to recruit and activate iNKT cells after ARDS induction.** WT, IL-$33^{-/-}$, and $ST2^{-/-}$ mice were subjected to a sham treatment or intratracheal LPS injection. After 24 h, the lung and spleen were obtained to prepare single-cell suspensions, and the cells were stained with anti-CD45, anti-CD3, anti-CD1d-tetramer, anti-NK1.1, anti-CD4, anti-CD8, and anti-CD69 antibodies. A and B, Representative dot plots. iNKT cells were identified as $CD45^+CD3^+CD1d^+$ tetramers (n = 5). C, The data are presented as the ratio of iNKT to $CD3^+$ T cells and the CD69 geometric mean expression on iNKT cells in the lung and spleen (n = 3–5). D and E, Representative dot plots. NK cells were identified as $CD45^+CD3^-NK1.1^+$ cells. F, The data are presented as the ratio of NK cells to $CD3^-$ T cells and CD69 geometric mean expression on NK cells in the lung and spleen (n = 3–5). Three independent experiments were conducted to obtain the results shown. The data are shown as the mean + SD. $^*P < 0.05$, $^{**}P < 0.01$, $^{***}P < 0.001$, $^{****}P < 0.0001$, and n. s., not significant. ARDS, acute respiratory distress syndrome; Ctr, control; KO, knockout; WT, wild-type.

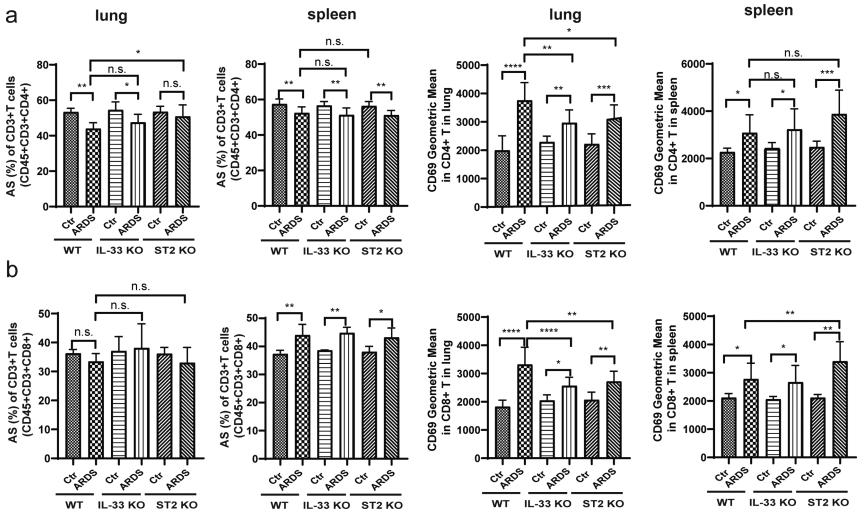

FIG. 5. **The ratio of CD4$^+$ T cells and CD8$^+$ T cells to CD3$^+$ T cells was not different after ARDS induction in IL-33$^{-/-}$ and ST$^{-/-}$ mice.** The lung and spleen were obtained to prepare single-cell suspensions, and the cells stained with anti-CD45, anti-CD3, anti-CD1d-tetramer, anti-NK1.1, anti-CD4, anti-CD8, and anti-CD69 antibodies 24 h after LPS-induced ARDS. A, The data are presented as the ratio of CD4$^+$ T cells to CD3$^+$ T cells and the CD69 geometric mean in CD4$^+$ T cells in the lung and spleen (n = 5). B, The data are presented as the ratio of CD8+ T cells to CD3$^+$ T cells and the CD69 geometric mean expression on CD8$^+$ T cells in the lung and spleen (n = 5). The results shown are based on one of three independent experiments. The data are shown as the mean + SD. *$P < 0.05$, **$P < 0.01$, ***$P < 0.001$, ****$P < 0.0001$, and n. s., not significant. ARDS, acute respiratory distress syndrome; ctr, control; KO, knockout; WT, wild-type.

surface expression of CD69 on CD8$^+$ T cells (Fig. 5B) was upregulated in the lung and spleen in the LPS-induced ARDS group. Moreover, IL-33 and ST2 deficiency significantly decreased the geometric mean of CD69 expression in the spleen and lung (Fig. 5B). However, no difference in the ratio of CD8$^+$ T cells to CD3$^+$ T cells in the lung or spleen of IL-33– or ST2-deficient mice was found (Fig. 5(B)).

iNKT cells promote lung injury

A significant reduction in iNKT cells was observed in mice lacking IL-33 or ST2. To explore the role of NKT cells in ARDS, we used CD1d$^{-/-}$ and Vα14Tg mice. As shown in Figure 6A–C, the ratio of D/W decreased, and the total protein concentration and neutrophil infiltration were increased in the BALF after LPS-induced ARDS, which indicated alveolar capillary leakage

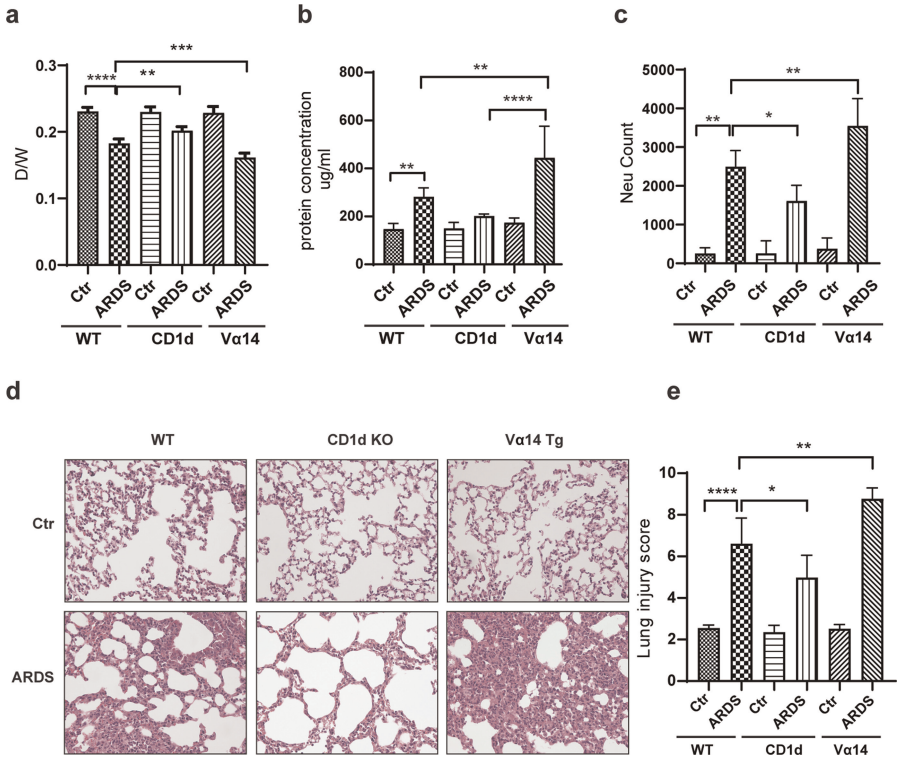

FIG. 6. **NKT cells contribute to lung injury in ARDS.** BALF and lung tissue were harvested 24 h after intratracheal LPS injection. A, The D/W ratio was recorded to evaluate lung edema (n = 5). Protein concentration (B) and neutrophil count (C) in the BALF were measured with a BCA kit and flow cytometry to determine epithelial permeability (n = 5). D and E, One representative image of five histological images (HE staining) of lung tissues. The lung injury score was evaluated by two pathologists blinded to the groups. Scale bar = 50 μm. The data are shown as the mean + SD. *$P < 0.05$, **$P < 0.01$, ***$P < 0.001$, ****$P < 0.0001$, and n. s., not significant. ARDS, acute respiratory distress syndrome; BALF, bronchoalveolar lavage fluid; ctr, control; D/W, dry/wet; HE, hematoxylin-eosin; KO, knockout; WT, wild-type.

and pulmonary edema. The D/W ratio was significantly increased in the CD1dKO group but decreased in Vα14Tg group compared with the WT group ($P < 0.05$) (Fig. 6A). However, the total protein concentration and neutrophil count in the BALF decreased in the CD1dKO group but significantly increased in the Vα14Tg group ($P < 0.05$) (Fig. 6, B–C).

Simultaneously, compared with that in the control group, lung injury in the ARDS group was much more severe, which manifested as increased leukocyte infiltration, alveolar congestion/hemorrhage, alveolar collapse, and thickened alveolar walls (Fig. 6D). However, the CD1d ARDS group showed less inflammatory injury than the LPS group, with the lung injury score significantly decreased in the former. In contrast, the alveoli congestion and hemorrhage, number of lung-infiltrating inflammatory cells, and lung injury scores in the V14g ARDS group were higher than those in the WT ARDS group (Fig. 6, D–E).

NKT cells contribute to cytokine secretion

In addition, IL-6, MCP-1, and TNF protein levels were measured in the BALF and serum as part of our assessment of the role of NKT cells in ARDS systemic inflammation. As expected, LPS-induced ARDS resulted in marked increases in IL-6, MCP-1, and TNF both in the plasma (Fig. 7A) and BALF (Fig. 7B) after 24 h. The levels of these cytokines were significantly higher in Vα14Tg mice during the first 24 h after ARDS induction. However, the serum and BALF levels of IL-6, MCP-1, and TNF were not different in CD1d-KO mice (Fig. 7, A–B).

IL-33 promotes the inflammatory response depending on NKT cells

Finally, to validate that IL-33 promotes inflammation through NKT cells, a neutralizing anti-ST2 antibody was administered to LPS-treated WT and Vα14Tg mice 1 h before LPS administration. As shown in Figure 8, the Vα14Tg mice showed increased alveolar-capillary leakage and pulmonary edema, which manifested as an increased total protein concentration and neutrophil infiltration in the BALF ($P < 0.05$) (Fig. 8, B–C) and a decreased D/W ratio ($P < 0.05$) (Fig. 8A), compared with those in the WT mice. In addition, compared with that in the WT ARDS group, the lung injury severity was higher in the Vα14Tg ARDS group (Fig. 8E), which manifested as increased leukocyte infiltration, alveolar congestion/hemorrhage, and alveolar collapse and thickened alveolar walls (Fig. 8D). This change in lung injury was accompanied by significant increases in plasma (Fig. 8F) and BALF (Fig. 8G) protein concentrations of cytokines (IL-6 and TNF-α) and a chemokine (MCP-1) in Vα14Tg mice subjected to LPS-induced ARDS compared with the levels in WT mice.

DISCUSSION

The results of our study indicate that IL-33 was released during the early stages of uncontrolled inflammation, which was validated 1 h after ARDS, and that IL-33 exerted a deleterious effect by targeting NKT cells in ARDS.

In humans, IL-33 is constitutively expressed in endothelial cells, epithelial cells, and stromal cells (21) in many organs, such as the lung stomach, liver, and kidney. In mouse lung tissue, alveolar epithelial cells express IL-33, and pulmonary vascular endothelial cells do not express IL-33 (22). Our immunohistochemical results confirmed that alveolar type 2 cells expressed IL-33. This finding was also reported by Li et al. (23). Although IL-33 is constitutively expressed, it is also regulated under different physiological and pathological circumstances. Our results showed that the transcript levels of IL-33 were also significantly elevated in lung tissue. This outcome suggests that the source of IL-33 may be induced and released from dying cells. This finding has also been reported in other

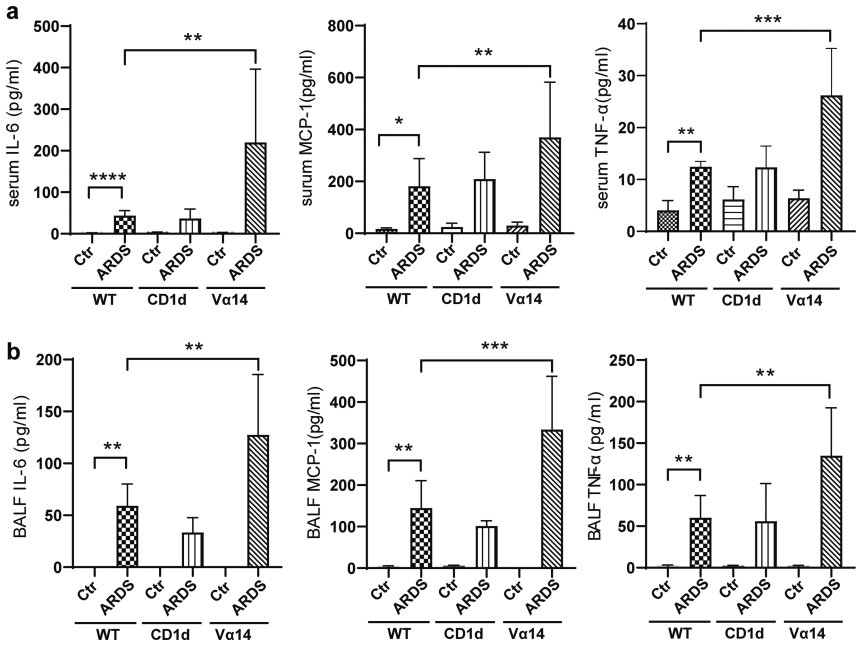

FIG. 7. **Activated NKT cells promote the release of inflammatory factors in the plasma and BALF.** The concentration of cytokines in the BALF was determined 24 h after ARDS induction by CBA. The IL-6, MCP-1, and TNF levels in the plasma (A) or BALF (B) of the WT mice, $CD1d^{-/-}$ mice and Vα14Tg mice were measured to evaluate the systemic inflammatory response (n = 5). The data are shown are the mean + SD. $^{*}P < 0.05$, $^{**}P < 0.01$, $^{***}P < 0.001$, and $^{****}P < 0.0001$. ARDS, acute respiratory distress syndrome; BALF, bronchoalveolar lavage fluid; ctr, control; KO, knockout; WT, wild-type.

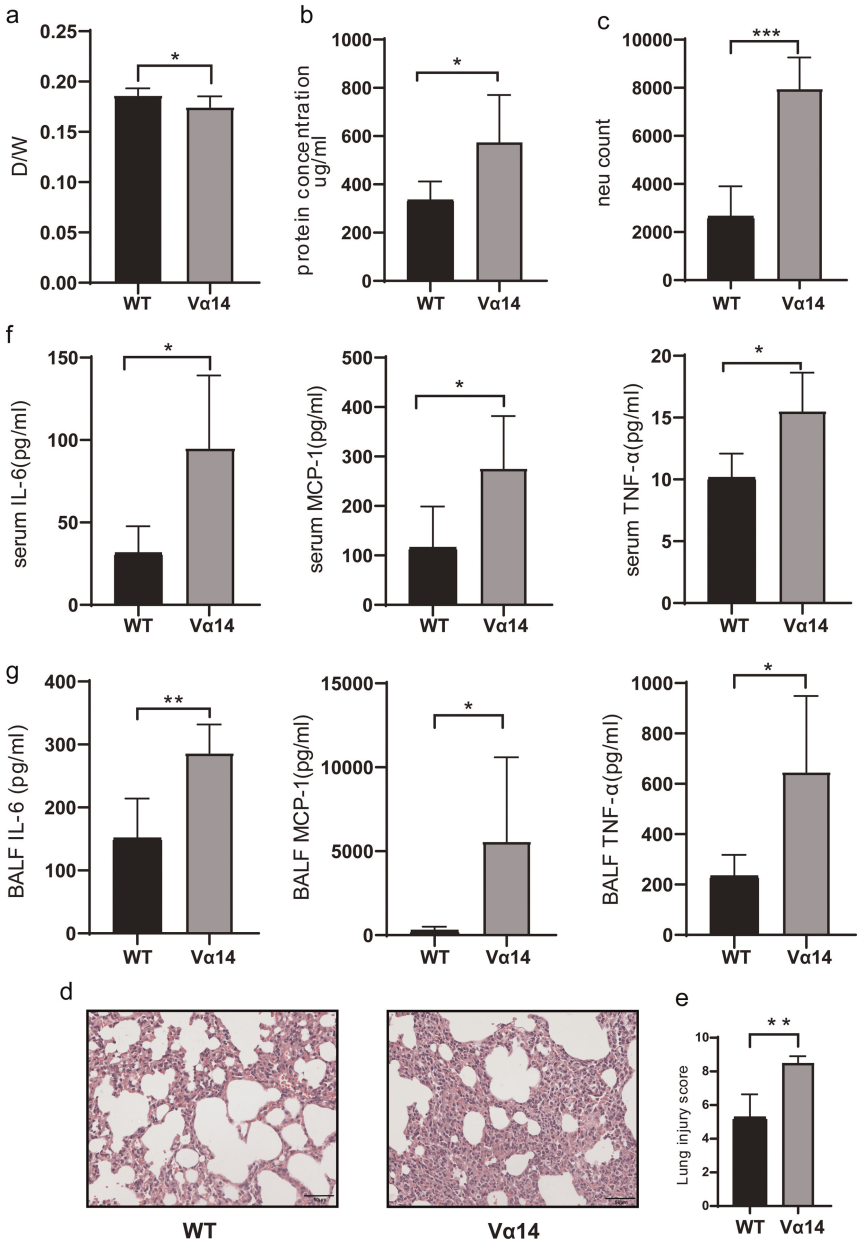

FIG. 8. **IL-33 contributes to an uncontrolled inflammatory response in ARDS *via* activation of NKT cells.** WT and Vα14Tg mice were pretreated with an anti-ST2 antibody 1 h before LPS administration and sacrificed 24 h after ARDS induction. BALF and lung tissue were harvested. A, The D/W ratio was calculated to evaluate lung edema (n = 5). B, Protein concentration and neutrophil count (C) in the BALF were measured with a BCA kit and by flow cytometry to evaluate epithelial permeability (n = 5). D and E, One of five representative histopathological images showing the lung tissues (HE staining). The lung injury score was determined by two blinded pathologists. Scale bar = 50 μm. F, The levels of IL-6, MCP-1, and TNF in the plasma and BALF were tested by CBA. (n = 5, *$P < 0.05$). The data are shown as the mean ± SD and are representative of three independent experiments. *$P < 0.05$, **$P < 0.01$, and ***$P < 0.001$. ARDS, acute respiratory distress syndrome; BALF, bronchoalveolar lavage fluid; ctr, control; D/W, dry/wet; KO, knockout; WT, wild-type.

diseases, such as asthma (24) and chronic obstructive pulmonary disease (25), in which the levels of IL-33 were found to be increased. In contrast to Thierry's findings (20), no significant differences were found in the transcript levels of IL-33 released into the kidney during the early phase of ischemia reperfusion. This outcome may be due to the difference between the lung and kidney tissue.

IL-33, similar to HMGB1, is rapidly passively released from damaged necrotic cells as an "alarmin" (26), alerting the immune system to respond to cell or tissue damage. This characteristic suggests that IL-33 may exert its cytokine effect at an early stage after disease onset. Indeed, the full-length form of IL-33 is released into the extracellular space after only 5 min of endothelial cell challenge with Alternaria extracts (27). In addition, *in vivo* exposure to PLA2 allergen for 15–30 min was sufficient to cause IL-33 release in mice (27). The precise release time of IL-33 has not yet been determined. Recently, clinical studies have collected serum samples within 24 h of admission, and patients with COVID-19 showed elevated IL-33 levels (9). In animal studies, 10 h after CLP, IL-33 levels were significantly elevated in the lungs and plasma (23). These results are different from our findings, which showed that IL-33 was significantly elevated 1 h after LPS-induced ARDS and decreased quickly, within 24 h. This result confirmed our supposition and agrees with Thierry's observations (20), which showed that IL-33 was released 1 h after IRI. Moreover,

it validates the idea that IL-33 modulates the immune response at an early stage of disease.

IL-33 is mainly found in the nucleus and is a transcription factor in addition to a cytokine. Both clinical and animal studies have validated that it exerts a deleterious effect on the uncontrolled inflammatory response in ARDS (9,28–30). This outcome is consistent with our findings, in which we used genetic engineering techniques to confirm that blocking the IL-33/ST2 axis attenuates early uncontrolled pulmonary edema and reduce proinflammatory factor release in ARDS mice. These outcomes suggest that we can modulate the uncontrolled inflammatory response of ARDS early using IL-33 monoclonal antibodies in the future. Currently, IL-33 monoclonal antibodies are available for the treatment of uncontrolled inflammatory responses in ARDS, but the expected clinical results have not been obtained (31). Combined with the findings of our experiment, it may be more effective to administer IL-33 monoclonal antibodies at a much earlier stage of ARDS.

As soon as it is secreted, IL-33 binds to a specific membrane receptor, ST2L, which belongs to the superfamily of receptors that are similar to those of the IL-1 receptor family. A wide variety of cellular targets express the ST2L receptor, notably immune cells such as the intrinsic immune cells ILC, NK, NKT, macrophages, neutrophils, and $CD4^+$ T cells, $CD8^+$ T cells, and Treg. Hence, it is worthwhile to further explore the main effector cells regulated by IL-33 in the early inflammation stage of ARDS. IL-33 targets NKT cells but not NK, CD4+ T cells, or CD8+ T cells, according to our study. NKT cell recruitment and activation in the lung were significantly reduced in mice deficient in IL-33 or ST2. To confirm the correlation between IL-33 and NKT cells, we designed reversal experiments using WT and Vα14Tg mice with prior blockade of IL-33 activation by an ST2 Fc chimera and found that IL-33 regulated the early uncontrolled inflammatory response that was dependent on NKT cells in ARDS. This was consistent with the result showing that IL-33 promoted the recruitment and activation of NKT cells at local injury sites within 24 h of IRI (20). IL-33 promotes an uncontrolled inflammatory response in ARDS by means of a newly discovered mechanism. It provides targetable molecules and immune cells for exploring the early uncontrolled inflammatory response in ARDS.

A previously unknown mechanism by which the IL-33/ST2 signaling axis regulates the early uncontrolled inflammatory response in ARDS in an NKT cell–dependent manner was revealed in this study using genetic mice and reversal experiments. Our work has the following important limitations: the IL-33/ST2 axis affected the activation indicator of conventional T lymphocytes, but the percentage has no difference. Further experiments are needed to explore the specific types of lymphocyte activation that play a role. In addition, we found that the IL-33/ST2 signaling axis regulates the early uncontrolled inflammatory response in ARDS in an NKT cell–dependent manner. However, unfortunately, we still do not know how IL-33 regulates the function of NKT cells. Thus, this issue will be explored in the future.

CONCLUSIONS

In summary, according to our data, IL-33 was released in ARDS at an early stage. In addition, we demonstrated that IL-33 stimulates the uncontrolled inflammatory response through iNKT cells. IL-33 and NKT cells may be molecules and immune cells, respectively, to target early for treating ARDS cytokine storms.

ACKNOWLEDGMENTS

The authors thank Professor Zheng Fang and Weng Xiufang for the gift of Vα14Tg, $CD1d^{-/-}$, IL-$33^{-/-}$, and $ST2^{-/-}$ mice.

REFERENCES

1. Bellani G, Laffey JG, Pham T, et al. Epidemiology, patterns of care, and mortality for patients with acute respiratory distress syndrome in intensive care units in 50 countries. *JAMA*. 2016;315(8):788–800.
2. Chen W, Chen YY, Tsai CF, et al. Incidence and outcomes of acute respiratory distress syndrome a nationwide registry-based study in Taiwan, 1997 to 2011. *Medicine*. 2015;94(43):e1849.
3. Cayrol C, Girard J-P. Interleukin-33 (IL-33): a nuclear cytokine from the IL-1 family. *Immunol Rev*. 2018;281(1):154–168.
4. Han P, Mi W-L, Wang Y-Q. Research progress on interleukin-33 and its roles in the central nervous system. *Neurosci Bull*. 2011;27(5):351–357.
5. Liew FY, Pitman NI, McInnes IB. Disease-associated functions of IL-33: the new kid in the IL-1 family. *Nat Rev Immunol*. 2010;10(2):103–110.
6. Lin SH, Fu J, Wang CJ, et al. Inflammation elevated IL-33 originating from the lung mediates inflammation in acute lung injury. *Clin Immunol*. 2016;173:32–43.
7. Stanczak MA, Sanin DE, Apostolova P, et al. IL-33 expression in response to SARS-CoV-2 correlates with seropositivity in COVID-19 convalescent individuals. *Nat Commun*. 2021;12(1):2133.
8. Zizzo G, Cohen PL. Imperfect storm: is interleukin-33 the Achilles heel of COVID-19? *Lancet Rheumatol*. 2020;2(12):E779–E790.
9. Kassianidis G, Siampanos A, Poulakou G, et al. Calprotectin and imbalances between acute-phase mediators are associated with critical illness in COVID-19. *Int J Mol Sci*. 2022;23(9):4894.
10. Halat G, Haider T, Dedeyan M, et al. IL-33 and its increased serum levels as an alarmin for imminent pulmonary complications in polytraumatized patients. *World J Emerg Surg*. 2019;14:36.
11. Burke H, Freeman A, Cellura DC, et al. Inflammatory phenotyping predicts clinical outcome in COVID-19. *Respir Res*. 2020;21(1):245.
12. Liu Q, Dwyer GK, Zhao Y, et al. IL-33–mediated IL-13 secretion by ST2+ Tregs controls inflammation after lung injury. *JCI Insight*. 2019;4(6):e123919.
13. Xu H, Xu J, Xu L, et al. Interleukin-33 contributes to ILC2 activation and early inflammation-associated lung injury during abdominal sepsis. *Immunol Cell Biol*. 2018;96(9):935–947.
14. Xu J, Guardado J, Hoffman R, et al. IL33-mediated ILC2 activation and neutrophil IL5 production in the lung response after severe trauma: a reverse translation study from a human cohort to a mouse trauma model. *PLoS Med*. 2017;14(7):e1002365.
15. Zarobkiewicz MK, Morawska I, Michalski A, et al. NKT and NKT-like cells in autoimmune neuroinflammatory diseases—multiple sclerosis, myasthenia gravis and Guillain-Barre syndrome. *Int J Mol Sci*. 2021;22(17):9520.
16. Rostan O, Arshad MI, Piquet-Pellorce C, et al. Crucial and diverse role of the Interleukin-33/ST2 axis in infectious diseases. *Infect Immun*. 2015;83(5):1738–1748.
17. Thierry A, Giraud S, Robin A, et al. The Alarmin concept applied to human renal transplantation: evidence for a differential implication of HMGB1 and IL-33. *PloS One*. 2014;9(2):e88742.
18. Albacker LA, Chaudhary V, Chang YJ, et al. Invariant natural killer T cells recognize a fungal glycosphingolipid that can induce airway hyperreactivity. *Nat Med*. 2013;19(10):1297–1304.
19. Bourgeois E, Van LP, Samson M, et al. The pro-Th2 cytokine IL-33 directly interacts with invariant NKT and NK cells to induce IFN-gamma production. *Eur J Immunol*. 2009;39(4):1046–1055.
20. Ferhat M, Robin A, Giraud S, et al. Endogenous IL-33 contributes to kidney ischemia-reperfusion injury as an alarmin. *J Am Soc Nephrol*. 2018;29(4):1272–1288.
21. Moussion C, Ortega N, Girard J-P. The IL-1-like cytokine IL-33 is constitutively expressed in the nucleus of endothelial cells and epithelial cells in vivo: a novel 'alarmin'? *PLoS One*. 2008;3(10):e3331.
22. Pichery M, Mirey E, Mercier P, et al. Endogenous IL-33 is highly expressed in mouse epithelial barrier tissues, lymphoid organs, brain, embryos, and inflamed tissues: in situ analysis using a novel IL-33-LacZ gene trap reporter strain. *J Immunol*. 2012;188(7):3488–3495.
23. Ding X, Jin S, Shao Z, et al. The IL-33-ST2 pathway contributes to ventilator-induced lung injury in septic mice in a tidal volume-dependent manner. *Shock*. 2019;52(3):E1–E11.

24. Al-Sajee D, Sehmi R, Hawke TJ, et al. Expression of IL-33 and TSLP and their receptors in asthmatic airways after inhaled allergen challenge. *Am J Respir Crit Care Med*. 2018;198(6):805–807.
25. Byers DE, Alexander-Brett J, Patel AC, et al. Long-term IL-33–producing epithelial progenitor cells in chronic obstructive lung disease. *J Clin Invest*. 2013; 123(9):3967–3982.
26. Bianchi ME. DAMPs, PAMPs and alarmins: all we need to know about danger. *J Leukoc Biol*. 2007;81(1):1–5.
27. Cayrol C, Duval A, Schmitt P, et al. Environmental allergens induce allergic inflammation through proteolytic maturation of IL-33. *Nat Immunol*. 2018;19(4): 375–385.
28. Fali T, Aychek T, Ferhat M, et al. Metabolic regulation by PPARγ is required for IL-33–mediated activation of ILC2s in lung and adipose tissue. *Mucosal Immunol*. 2020;14(3):585–593.
29. Lei M, Wang CJ, Yu F, et al. Different intensity of autophagy regulate interleukin-33 to control the uncontrolled inflammation of acute lung injury. *Inflamm Res*. 2019; 68(8):665–675.
30. Zhang Y, Lv R, Hu X, et al. The role of IL-33 on LPS-induced acute lung injury in mice. *Inflammation*. 2017;40(1):285–294.
31. Patel S, Saxena B, Mehta P. Recent updates in the clinical trials of therapeutic monoclonal antibodies targeting cytokine storm for the management of COVID-19. *Heliyon*. 2021;7(2):e06158.